



ACADEMIC
PRESS

Available online at www.sciencedirect.com

SCIENCE @ DIRECT®

Journal of Sound and Vibration 271 (2004) 985–998

JOURNAL OF
SOUND AND
VIBRATION

www.elsevier.com/locate/jsvi

Measurement of large harmonic vibration amplitudes

A. Mozuras^{a,b,*}, E. Podzharov^{b,c}

^a *Research Laboratory Akustika, Muitines 13-57, Vilnius 2006, Lithuania*

^b *University of Guadalajara, AV. Revolucion 1500, Puerta 10, Guadalajara C.P. 44430 Jal., Mexico*

^c *University of Panamericana, Prol. Calz. Circunv. Pte. 49, Cd. Granja, Zapopan C.P. 45010, Jal., Mexico*

Received 25 October 2002; accepted 12 March 2003

Abstract

The greater the linearity of a transducer, the more suitable it is for vibration measurement. However, purely linear transducers are not available. It is very common to only use a transducer in a narrow range, where its converting characteristic is close to linear. Unfortunately, only a low signal level can thus be obtained. Therefore, the use of linear features in the measurement process causes non-linear distortions as well as a low signal-to-noise ratio. In this paper, a method for measurement of harmonic vibration amplitudes is presented that allows one to eliminate the above drawbacks. This method allows the extension of the range available for vibration measurement. It could be used, for example, in measurement of standing waves, calibration of devices, etc. This method also gives the ability to obtain maps of the vibration amplitudes with increased surface resolution.

© 2003 Elsevier Ltd. All rights reserved.

1. Introduction

Vibration characteristics are very important for many products in the manufacturing industry. The classical vibration measurement methods are usually based on mechanical contact. Over the past decade, non-contact methods (e.g., optical methods) have been developed for industrial applications. With the characteristic of non-destructiveness, these methods are widely used in industry for manufacturing process and automation.

In conventional vibration measurement methods, a physical converter is considered more suitable for measurement purposes when its linearity is greater. However, purely linear converting systems are not available. Practically, each non-linear converter can be considered as linear when an output signal level is very small. In this case, influence of noise is increased significantly and

*Corresponding author. Almantas Mozuras, Muitines 13-57, 2006 Vilnius, Lithuania.

E-mail address: alma@ktl.mii.lt, amozuras@netscape.net (A. Mozuras).

signal-to-noise ratio is decreased. When trying to increase an output level, non-linear distortions increase simultaneously [1–3].

The non-linearities may be treated by artificial linearization [4]. This method uses an additional converter following the principal one with an inverse converting function to that of the primary displacement converter to compensate for the non-linear distortions. Usually, this method extends the measurement range to a very limited degree.

Thus, the use of the linear features in a vibration measurement process finally causes a systematic error due to non-linear distortions, low signal-to-noise ratio, and low surface resolution. To eliminate the above drawbacks a method of measurement of harmonic vibration amplitudes has been created. Advantages of this method are shown when using electric, electrostatic, inductive, and photoelectric transducers. However, this method is not limited to these transducers. Transducers that could not be used because of great non-linearity can now be used because of this method. Theoretical conclusions are accompanied by the experimental results.

2. Description of the method

Suppose a non-contact transducer has a non-linear characteristic $f(x)$, where x is the distance between an object and the transducer head. Assume the object vibrates harmonically with the cyclic frequency ω and an amplitude x_0 to be measured (Fig. 1). Thus, the instant distance is

$$x = \bar{x} + x_0 \cos \omega t, \quad (1)$$

where \bar{x} is the average distance. According to the new method, the transducer is located at the minimum distance from the vibrating object so that it is not touching a surface of the object. During the measurement process, an output signal of the transducer $f(x(t))$ is registered. The output signal is differentiated with respect to time and the differentiated signal may be written as

$$\psi = \frac{df(x)}{dx} \frac{dx}{dt}. \quad (2)$$

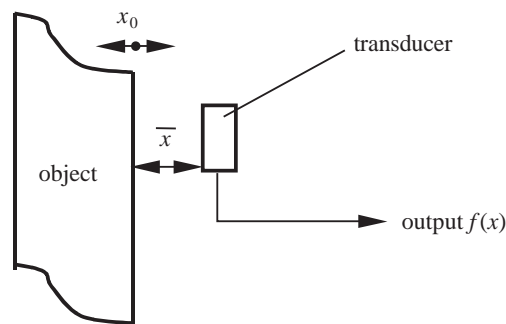
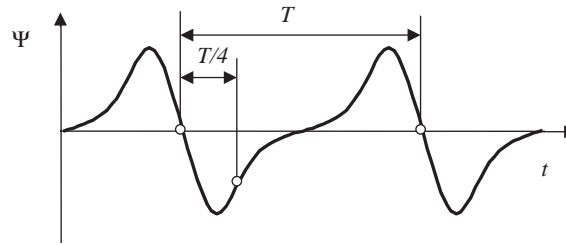


Fig. 1. General scheme of the method.

Fig. 2. Typical signal Ψ .

Denoting $F(x) = df(x)/dx$ Eq. (2) can be rewritten as

$$\Psi = F(x) \frac{dx}{dt}. \quad (3)$$

If x varies according to Eq. (1), then the function describing changes of signal (3) in time is

$$\Psi = -F(\bar{x} + x_0 \cos(\omega t)) \omega x_0 \sin(\omega t). \quad (4)$$

A period T of the signal Ψ is determined. The signal value is measured $T/4$ after the signal crosses zero (Fig. 2). The latter signal value multiplied by the period T gives an estimate of the vibration amplitude.

The essence of this method consists of the following. The function $F(x)$ increases strongly with decrease in x . Dependence of the signal values measured at the time instants

$$\omega t = \pi/2 + \pi k, \quad (k = 0, 1, 2, \dots), \quad (5)$$

on the amplitude x_0 is linear:

$$\Psi(\pi/2 + \pi k) = \pm F(\bar{x}) \frac{2\pi}{T} x_0. \quad (6)$$

Therefore, the systematic error due to non-linear distortions is excluded. This allows one to reduce the distance \bar{x} between the transducer and the vibrating object. Therefore, at the minimum distance \bar{x} the information signal Ψ and signal-to-noise ratio reach their maximum values.

The amplitude is equal to

$$x_0 = CT\Psi(\pi/2 + \pi k), \quad (7)$$

where C is the proportionality constant.

3. Errors

The converting function (3) is characteristic for velocity transducers. The structural schemes of the electrostatic and electretic [5] transducers are given in Figs. 3a and b, respectively. When the object vibrates, both transducers act as dynamic capacitors. A difference is that the first one uses the constant electric voltage source and the second one uses the electrically charged electretic film. When $T \gg RC$, where C and R are the dynamic capacitor and the load resistance, respectively, both transducers could be considered as velocity transducers. In the case of the electrostatic transducer, the electric charge accumulated on the electrode of the dynamic

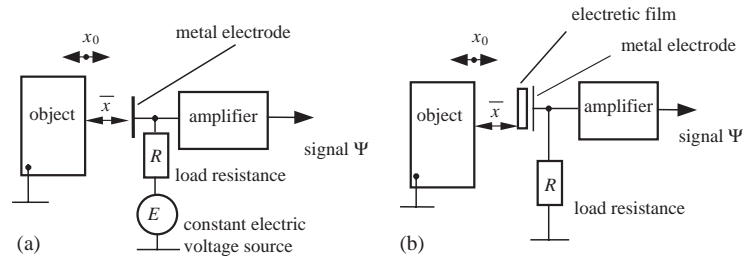


Fig. 3. Structural scheme of the electrostatic (a) and electretic (b) transducer.

capacitor is equal to

$$Q(x) = E \frac{\epsilon_a S}{x}, \tag{8}$$

where E , ϵ_a , S are the electromotive force, absolute dielectric permittivity of the environment, and the area of the electrode, respectively. In the case of the electretic converter, the charge density induced on the object surface by the electret is expressed as [5]

$$\sigma_{ind}(x) = -\frac{\sigma}{(\epsilon x/L) + 1} = -\frac{\sigma L/\epsilon}{(x + L/\epsilon)}, \tag{9}$$

where σ , L , ϵ are the surface charge density, thickness, and permittivity of the electret, respectively. The information signal Ψ is the current that in the first case is equal to $dQ(x)/dt$ and in the second case to $Sd\sigma_{ind}(x)/dt$ (where S is the area of the metal electrode, see Fig. 3b). In both cases the signal Ψ is $\Psi = Bx_0^{-1}(A + \cos \omega t)^{-2} \sin \omega t$. The quantities A and B for the electretic transducer are equal to

$$\begin{aligned} A &= (\bar{x} + L/\epsilon)/x_0, \\ B &= -RLS\sigma\omega/\epsilon \end{aligned} \tag{10}$$

and for the electrostatic transducer

$$\begin{aligned} A &= \bar{x}/x_0, \\ B &= RES\omega\epsilon_a, \end{aligned} \tag{11}$$

where $A > 1$, R is the load resistance and S is the area of the metal electrode.

In the following, an application of the method is given using a photoelectric transducer [6] (Fig. 4). This transducer is based on registration of light rays reflected from the object surface. It consists of a light emitting diode and a photodiode. The light emitting diode and the photodiode are considered as a point light source and receiver, respectively. They are both placed close one to another near the object surface of which the vibration amplitude is to be measured. In this case, the transducer output signal $f(x)$ is a photodiode current (or a registered light intensity) which follows the inverse square law if the distance x is large compared to the diameter of the light source and that of the light receiver

$$f(x) = \frac{C_e}{x^2}, \tag{12}$$

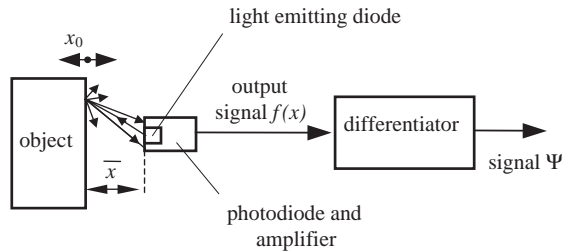


Fig. 4. Structural measurement scheme using the photoelectric transducer.

where C_e is some constant of the photoelectric transducer. According to its nature, the photoelectric transducer does not provide differentiation of the function $f(x)$. Thus, it is necessary to perform the differentiation artificially. The differentiated signal is $\Psi = 2C_e x_0^{-2} (A + \cos \omega t)^{-3} \sin \omega t$, where the quantity A is relative average distance ($A = \bar{x}/x_0$, $A > 1$).

Characteristics (8), (9) and (12) could be written in the general form

$$f(x) = \frac{C}{x^n}, \tag{13}$$

where the power n is equal to 1 for the electrostatic and the electretic, and to 2 for the photoelectric transducer. In the case of the electretic transducer the quantity $x + L/\epsilon$ is in the denominator of Eq. (13) instead of x ($n = 1$), however, the quantity L/ϵ could be included in \bar{x} as follows from Eqs. (1) and (13) used further.

In the following, errors of the conventional method, when the amplitude is obtained taking into account extreme values of the transducer output signal, will be calculated and compared with errors of the new method.

Evaluating the systematic error due to non-linear distortions, the output signal (3) can be written as

$$\Psi = -n \frac{C}{x^{n+1}} \frac{dx}{dt} = \frac{n\omega C}{(\bar{x})^n} \frac{A^n \sin(\omega t)}{(A + \cos(\omega t))^{n+1}}. \tag{14}$$

After solving the equation $d\Psi/dt = 0$ and substituting the extreme phase $(\omega t)_e$ back into Eq. (14), one obtains an expression for the extrema of the signal Ψ

$$\Psi_e = \pm \frac{2^{n+1/2} n^{n+1} \omega C A^n \left(A \sqrt{A^2 + 4n^2 + 4n} - A^2 - 2n \right)^{1/2}}{(\bar{x})^n \left(2An + A - \sqrt{A^2 + 4n^2 + 4n} \right)^{n+1}}. \tag{15}$$

The signal of the proposed method could be written as

$$\Psi(\pi/2 + \pi k) = \pm \frac{n\omega C}{(\bar{x})^n} \frac{1}{A}. \tag{16}$$

Error due to non-linear distortions that occurs in the conventional method is equal to

$$\left(\frac{\Delta x_0}{x_0} \right)_1 = \frac{\Psi_e - \Psi(\pi/2 + \pi k)}{\Psi(\pi/2 + \pi k)}, \tag{17}$$

or

$$\left(\frac{\Delta x_0}{x_0}\right)_1 = 2^{n+1/2} n^n A^{n+1} \frac{\left(A\sqrt{A^2 + 4n^2 + 4n} - A^2 - 2n\right)^{1/2}}{\left(2An + A - \sqrt{A^2 + 4n^2 + 4n}\right)^{n+1}} - 1, \tag{18}$$

and error due to noise could be calculated from the relation

$$\left(\frac{\Delta x_0}{x_0}\right)_2 = -\frac{\Delta A}{A} = -\frac{1}{(d\Psi_e/dA)A} \Delta\Psi_n = -\frac{\Psi_e|_{A=5}}{(d\Psi_e/dA)A} (\Delta\Psi_n/\Psi_e)|_{A=5}, \tag{19}$$

where $\Psi_e|_{A=5}$ is signal Ψ_e value in the point $A = 5$, $\Delta\Psi_n$ is uncertainty of Ψ_e due to noise, and $(\Delta\Psi_n/\Psi_e)|_{A=5}$ is relative noise error in $A = 5$. Substituting (15) into Eq. (19) one obtains

$$\left(\frac{\Delta x_0}{x_0}\right)_2 = \frac{2^{3/2} \frac{\left(5\sqrt{5^2+8}-5^2-2\right)^{1/2}}{\left(15-\sqrt{5^2+8}\right)^2}}{4\sqrt{2} \frac{\left(3A\sqrt{A^2+8}-A^2-8\right)}{\left(3A-\sqrt{A^2+8}\right)^3 \sqrt{A\sqrt{A^2+8}-A^2-2}\sqrt{A^2+8}}} \left(\frac{\Delta\Psi_n}{\Psi_e}\right)\Big|_{A=5}. \tag{20}$$

(Here only the error for $n = 1$ is presented due to the complicated expression required for any n). It should be mentioned that Eq. (20) is obtained from (19) substituting Ax_0 for \bar{x} after differentiation $d\Psi_e/dA$, and allows one to calculate dependence of the noise error on A (or \bar{x}) keeping $x_0 = const$ which is important by amplitude measurements. In the case of the conventional method when $n = 1$ (the electric or electrostatic transducer), curve 1 shows the dependence of the non-linear distortion error on the parameter A and curve 2 corresponds to the dependence of the noise error on A (Fig. 5). Error due to noise of this proposed method is

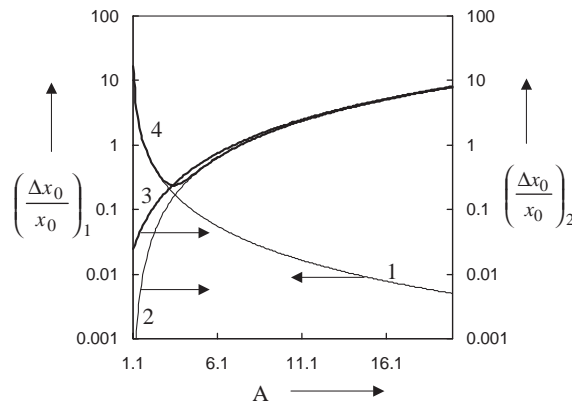


Fig. 5. Dependence of three factors on the parameter A in the conventional method: (1) the non-linear distortion error (curve 1), (2) the noise error (curve 2), (3) the combined (noise and distortion) error (curve 4). Curve 3 represents the dependence of noise error on A in this proposed method ($n = 1, (\Delta\Psi_n/\Psi_e)|_{A=5} = 0.05$).

found in the similar way and may be written as

$$\begin{aligned} \left(\frac{\Delta x_0}{x_0}\right)_2 &= -\frac{1}{(d\Psi(\pi/2)/dA)A} \Delta\Psi_n = -\frac{\Psi_e|_{A=5}}{(d\Psi(\pi/2)/dA)A} \left(\frac{\Delta\Psi_n}{\Psi_e}\right)\Bigg|_{A=5} \\ &= -\frac{2^{n+1/2}n^n \left(5\sqrt{5^2+4n^2+4n-5^2-2n}\right)^{1/2}}{(25n+5-\sqrt{5^2+4n^2+4n})^{n+1}} \left(\frac{\Delta\Psi_n}{\Psi_e}\right)\Bigg|_{A=5}. \end{aligned} \tag{21}$$

Curve 3 represents the dependence of the noise error on A . One can see that using the conventional method, it is not possible to decrease the error due to noise (curve 2) by decreasing the distance between the vibrating object and the transducer head. This is due to the increase of the non-linear distortion error (curve 1). In contrast, the proposed method allows one to decrease noise (curve 3) in such a way because the non-linear distortions are eliminated.

When using the photoelectric transducer ($n = 2$), the errors of the conventional measurement method are calculated considering the fact that in contrast to the previous case the output signal of the transducer is not differentiated. The amplitude x_0 is measured considering that it is proportional to half of the difference between the maximum and minimum values of the output signal. Thus, one can write for this difference:

$$\frac{(\Delta f)_{nonl}}{2} = \frac{1}{2} \left(\frac{C}{(\bar{x} - x_0)^2} - \frac{C}{(\bar{x} + x_0)^2} \right) = C \frac{2\bar{x}x_0}{(\bar{x}^2 - x_0^2)^2}, \tag{22}$$

and in the linear approach $x_0^2 \rightarrow 0$:

$$\frac{(\Delta f)_{lin}}{2} = C \frac{2x_0}{\bar{x}^3}. \tag{23}$$

The error due to non-linear distortions is equal to

$$\left(\frac{\Delta x_0}{x_0}\right)_1 = \frac{(\Delta f)_{nonl}/2 - (\Delta f)_{lin}/2}{(\Delta f)_{lin}/2} = \frac{A^4}{(A^2 - 1)^2} - 1. \tag{24}$$

The error due to noise can be written as

$$\left(\frac{\Delta x_0}{x_0}\right)_2 = \frac{((\Delta f)_{nonl}/2)|_{A=5}}{\frac{d((\Delta f)_{nonl}/2)}{dx_0} x_0} \left(\frac{\Delta f_n}{(\Delta f)_{nonl}/2}\right)\Bigg|_{A=5} = \frac{5}{(5^2 - 1)^2} \frac{(A^2 - 1)^3}{A(A^2 + 3)} \left(\frac{\Delta f_n}{(\Delta f)_{nonl}/2}\right)\Bigg|_{A=5}, \tag{25}$$

where $(\Delta f_n/((\Delta f)_{nonl}/2))|_{A=5}$ is the relative noise error for $A = 5$. Calculation of the noise error of the proposed method is more complicated because of simultaneous differentiation of the noise caused by the differentiation of the signal. It is necessary to find relations between the not differentiated and the differentiated noise. Suppose measurements are perturbed by white noise. Spectral power density p of such noise is frequency independent [7]. In the sufficiently general way assuming uncertainty Δf_n is equal to a standard deviation of the noise, one can write for the noise error of the conventional method

$$\Delta f_n = \sqrt{\frac{1}{2\pi} \int_0^{\Delta\omega} p d\omega} = \sqrt{\frac{p\Delta\omega}{2\pi}}, \tag{26}$$

where $\Delta\omega$ is the angular frequency range used in measurements. If the noise, with spectral power density p , is differentiated with respect to time, the resulting spectral power density will be $\omega^2 p$ [7]. Noise error $\Delta\Psi_n$ of the proposed method could be written as

$$\Delta\Psi_n = \sqrt{\frac{1}{2\pi} \int_0^{\Delta\omega} \omega^2 p d\omega} = \sqrt{\frac{p(\Delta\omega)^3}{6\pi}} = \frac{\Delta\omega}{\sqrt{3}} \Delta f_n. \tag{27}$$

Taking into account Eq. (27) the noise error of the proposed method is

$$\left(\frac{\Delta x_0}{x_0}\right)_2 = \sqrt{3} \frac{5}{(5^2 - 1)^2} \frac{\Delta\omega}{\omega} A^3 \left(\frac{\Delta f_n}{(\Delta f)_{nonl}/2}\right) \Big|_{A=5}. \tag{28}$$

Curve 1 shows the dependence of the non-linear distortion error on the parameter A (Fig. 6), curve 2 the dependence of the noise error on A in the conventional method, and curve 3 the dependence of the noise error on A in the proposed method.

From Figs. 5 and 6 one can see that using the conventional method, it is not possible to decrease the error due to noise (curve 2) by decreasing the distance between the vibrating object and the transducer head. This is because the error increases due to non-linear distortions (curve 1). In contrast, the proposed method allows one to decrease noise (curve 3), because the non-linear distortions are avoided.

As it can be seen, the proposed method works better with smaller values of the parameter A . It is possible to find a critical ratio A_c such that for $A < A_c$, the error of the proposed method is smaller than the total error of the conventional method. The total error of the conventional method could be written in the form

$$\left(\frac{\Delta x_0}{x_0}\right)_{conv.m.} = \sqrt{\left(\frac{\Delta x_0}{x_0}\right)_1^2 + \left(\frac{\Delta x_0}{x_0}\right)_2^2}. \tag{29}$$

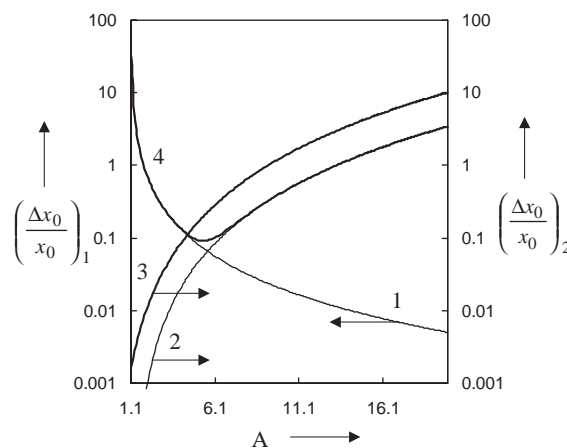


Fig. 6. Dependence of three factors on the parameter A in the conventional method: (1) the non-linear distortion error (curve 1), (2) the noise error (curve 2), (3) the combined (noise and distortion) error (curve 4). Curve 3 represents the dependence of noise error on A in this proposed method ($n = 2$, $[\Delta f_n / (\Delta f_{nonl} / 2)]_{A=5} = 0.05$, $\Delta\omega / \omega = 5$).

Its dependence on A represents curve 4 in Figs. 5 and 6. A condition for finding the critical ratio A_c is

$$\min \left[\left(\frac{\Delta x_0}{x_0} \right)_{conv.m.} \right] - \left(\frac{\Delta x_0}{x_0} \right)_{prop.m.} = 0, \tag{30}$$

where $(\Delta x_0/x_0)_{prop.m.}$ is the total error of the proposed method (or its noise error), and $\min[]$ is the function that means a minimum value of its argument. Curves 1 and 2 (Fig. 7) represent the dependence of the critical ratio A_c on the relative noise error found by numerical solution of Eq. (30) for the above-mentioned cases with $n = 1$ and 2, respectively. Nevertheless the noise is increased in the differentiation process, the critical ratio A_c is greater in the second case ($n = 2$). Also the reasonable measurement range found from condition $A < A_c$ is greater in this case.

Another problem is the measurement of the distribution of amplitudes on a surface. This arises when measuring vibrations of the objects with distributed parameters. An increase in the measurement resolution is possible by decreasing geometrical dimensions of the measuring head. However, it is related to the decrease of the signal level in the conventional measurement method. In the condition of a standing wave (see Fig. 8) the instant distance between the point s of the vibrating surface and the transducer head is equal to $x = \bar{x} + x_0(s) \cos \omega t$. For example, the output current of the electretic transducer could be calculated by integrating

$$i = \frac{d}{dt} \int \int_S \sigma_{ind}(s, t) ds, \tag{31}$$

where S is the area of the measuring electrode. Taking into account Eq. (9) the output signal in the proposed method may be written as

$$i(\pi/2 + \pi k) = \pm \frac{\omega \sigma L / \varepsilon}{(\bar{x} + L/\varepsilon)^2} S \bar{x}_0, \tag{32}$$

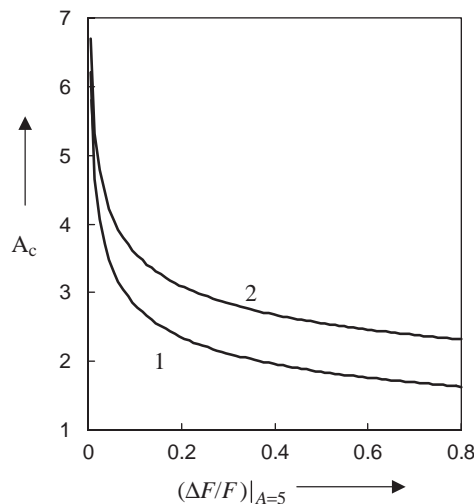


Fig. 7. Dependence of the critical ratio A_c on the relative noise error: curve 1 – $n = 1$, $(\Delta F/F)|_{A=5} = (\Delta \Psi_n / \Psi_e)|_{A=5}$, curve 2 – $n = 2$, $(\Delta F/F)|_{A=5} = [\Delta f_n / (\Delta f_{nonl}/2)]|_{A=5}$, $\Delta \omega / \omega = 5$.

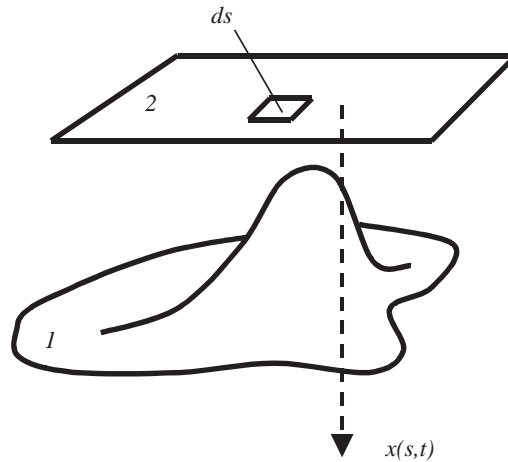


Fig. 8. Solving of the problem of increasing amplitude measurement resolution.

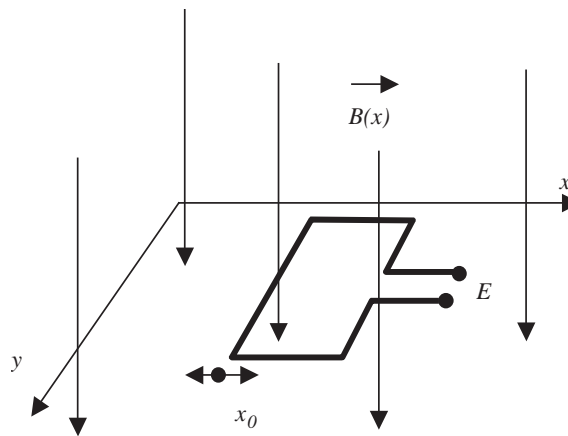


Fig. 9. Structural scheme of the induction transducer.

where $\bar{x}_0 = 1/S \int \int_S x_0(s) ds$ is the average measured amplitude. Since the non-linear distortions error is excluded, the proposed method allows one to increase the signal level by decreasing the distance \bar{x} and compensating in this way for influence of the decreased area S to improve the resolution as seen from Eq. (27).

An induction transducer [6] is shown in Fig. 9. A magnetic induction B is artificially made varying along the axis x , i.e., $B = B(x)$. Magnetic flux Φ intersecting the coil of wire consisting of m loops is calculated by integrating in the surrounded area

$$\Phi(x) = m\Delta y \int_x^{x+\Delta x} B(\xi) d\xi, \tag{33}$$

where Δx and Δy are geometrical dimensions of the coil along the directions x and y , respectively. The electromotive force in the circuit is

$$E = -\frac{d\Phi(x)}{dt} = -\frac{d\Phi(x)}{dx} \frac{dx}{dt} = -m\Delta y [B(x + \Delta x) - B(x)] \frac{dx}{dt} \tag{34}$$

As a result, one obtains a structure of Eq. (3). One could see, that for the proposed method to work the function $B(x)$ does not have any restrictions except that the function breaks. However, in order to determine the time instants $\omega t = \pi/2 + \pi k$ without difficulty the function should have a convenient characteristic, for example, to be monotonic.

4. Experiment

Experimental investigations of this method have been performed using the photoelectric transducer, analog-to-digital converter (ADC), and the computer connected in series (see Fig. 10). Harmonic vibration has been excited at the frequency $\omega/(2\pi) = 42$ Hz with the help of a vibrator.

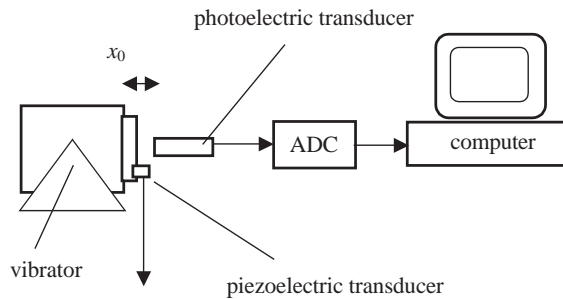


Fig. 10. Experimental scheme of the vibration amplitude measurement.

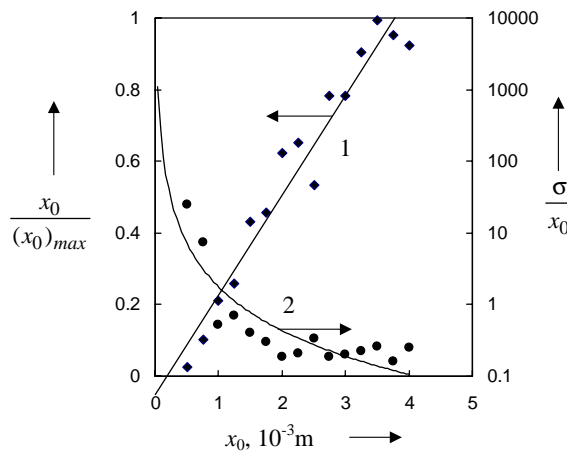


Fig. 11. Experimental dependence of the averaged measured amplitude (curve 1) and of the standard error (curve 2) on the given vibration amplitude obtained without using the frequency filter; $\bar{x} = 4.2 \times 10^{-3}$ m.

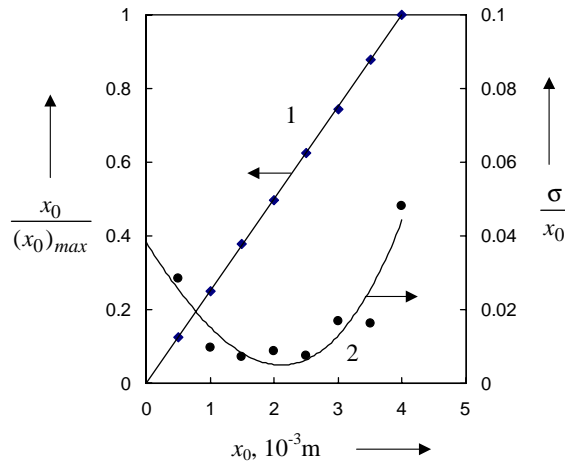


Fig. 12. Experimental dependence of the averaged measured amplitude (curve 1) and of the standard error (curve 2) on the given vibration amplitude obtained using the frequency filter; $\bar{x} = 4.2 \times 10^{-3} m$.

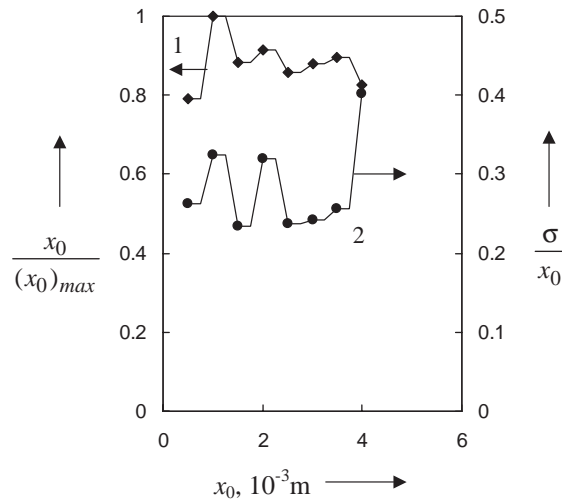


Fig. 13. Experimental dependence of the averaged measured amplitude (curve 1) and of the standard error (curve 2) on the given vibration amplitude obtained using a frequency filter in the conventional measurement method; $\bar{x} = 40 \times 10^{-3} m$.

Comparison of the proposed method with the conventional one in which the amplitude is considered to be proportional to the difference between the minima and the maxima of the measured signal could be made taking into account experimental curves shown in Figs. 11–13. In these figures, curve 1 represents experimental dependence of the averaged amplitude (measured using the proposed or the conventional method) on the amplitude x_0 measured with the help of the auxiliary contact piezoelectric transducer, and curve 2 represents the standard deviation. Curve 1 is obtained by increasing stepwise the vibration amplitude of the vibrator. Each point of

the curve 1 has been calculated from 10 amplitude measurements performed for each vibrator amplitude position. Curve 2 has been constructed by calculating the standard deviation σ using these 10 amplitude measurement results for each vibrator amplitude position and dividing σ by the corresponding averaged amplitude x_0 . Figs. 11 and 12 have been obtained at a distance of $\bar{x} = 4.2 \times 10^{-3}$ m and Fig. 13 at a distance of $\bar{x} = 40 \times 10^{-3}$ m because at this distance the non-linear error $(\Delta x_0/x_0)_1$ of the conventional method is less than 0.05 (see Fig. 6). In this proposed method, the required additional differentiation of the measured signal has been performed digitally. Denoting spectral components by Z_l , the output signal $f(x(t))$ of the transducer could be expressed in the form

$$f(x(t)) = \sum_{l=0}^{\infty} Z_l \cos l\omega t. \tag{35}$$

Differentiation of Eq. (35) with respect to t leads to

$$\Psi = -\omega \sum_{l=0}^{\infty} lZ_l \sin l\omega t, \tag{36}$$

and

$$\Psi(\pi/2) = -\omega \sum_{l=0}^{\infty} lZ_l \sin l\frac{\pi}{2} = -\omega \sum_{n=0}^{\infty} (-1)^n (2n + 1)Z_{2n+1}. \tag{37}$$

Taking into account Eq. (7) for the amplitude one obtains

$$x_0 \sim \sum_{n=0}^{\infty} (-1)^n (2n + 1)Z_{2n+1}. \tag{38}$$

The coefficients Z_l are proportional to the Fourier coefficients and have been found by performing the Fourier transform of the converter output signal $f(x(t))$. A filtration has been used to diminish the noise influence according to the condition

$$Z_l = \begin{cases} Z_l & \text{if } |Z_{l-1}| > |Z_l| \\ 0 & \text{if } |Z_{l-1}| \leq |Z_l| \end{cases}. \tag{39}$$

Comparing curves 1 in Figs. 11 and 12 one can see that the filtrated curve has a clearly expressed linear characteristic (standard error is $\sigma/x_0 < 0.05$) in contrast to the non-filtrated ($\sigma/x_0 < 25$). However, in the conventional method, as seen from Fig. 13, noise is so significant that any filtration cannot reduce the noise to an acceptable level ($\sigma/x_0 < 0.4$), and the useful signal is completely covered by the noise. It should be mentioned that in the latter case the signal level was about 1000 times smaller. As could be determined from Figs. 11 and 6, curves 2 have some similar characteristic, i.e. both curves decrease with a decrease of parameter A . However, curve 2 in Fig. 6 is obtained keeping $x_0 = const$ and for a more exact comparison of the curves it is necessary to recalculate curve 2 in Fig. 6 keeping \bar{x} constant ($\bar{x} = const$). When using filtration (Eq. (39)), the type of curve 2 is changed to quadratic (Fig. 12).

5. Conclusions

1. This proposed method allows one to measure the amplitude of the harmonic vibration with increased signal-to-noise ratio.

2. The error due to non-linear distortions is eliminated, which favours an increase in signal level by decreasing the distance between the object and the transducer head and increasing the resolution when the amplitude distribution on the surface of the vibrating object is measured.

3. Requirements for the converting characteristic $f(x)$ of the transducer are very few. It should not have any discontinuities. This method enables the use of transducers that have typically not been used because of great non-linearity.

References

- [1] R.V. Jones, J.C.S. Richards, The design and some applications of sensitive capacitance micrometers, *Journal of Physics* E6 (1973) 589–600.
- [2] K. Zhang, C. Butler, Q. Yang, Y. Lu, A fiber optic sensor for the measurement of surface roughness and displacement using artificial neural networks, *IEEE Transactions on Instrumentation and Measurement* 46 (4) (1997) 899–902.
- [3] A. Mozuras, K. Ragulskis, A method of displacement measurement, Certificate of Invention No. 1634986, Moscow, 1991.
- [4] DISA transducer manual. Incl. Type 51E01. Reg. N 9150 A 3211. DISA Electronic A/S, Herlev, Denmark.
- [5] G.M. Sessler, *Electrets, Topics in Applied Physics*, Vol. 33, Springer, Berlin, 1980.
- [6] J.P. Holman, *Experimental Methods for Engineers*, 6th Edition, McGraw-Hill, New York, 1994.
- [7] S.I. Baskakov, *RadiolEngineering Circuits and Signals*, Vysshaya Shkola, Moscow, 1988.